Collisional radiative model of a helium capillary glow discharge including atomic collisions

G. Gousset, C. Boulmer-Leborgne

J. Physique **45** (1984) 689-702 AVRIL **1984**, PAGE 689

Classification
Physics Abstracts
52.20F — 52.20H — 52.65

Collisional radiative model of a helium capillary glow discharge including atomic collisions

G. Gousset and C. Boulmer-Leborgne

Groupe de Recherche sur l'Energétique des Milieux Ionisés, CNRS, Université d'Orléans, U.E.R. Sciences Fondamentales et Appliquées, 45046 Orléans Cedex, France

(*Reçu le 27 mai 1983, révisé le 12 octobre, accepté le 15 décembre 1983*)

Résumé. — Un nouveau modèle collisionnel radiatif est développé en tenant compte des transferts d'excitation entre sous-niveaux d'un même état par collisions atomiques, de l'ionisation associative et des transferts d'excitation entre états de n différents ($n \geqq 8$). Ce modèle est utilisé pour déterminer la température électronique des plasmas à basse densité. Le domaine de validité du modèle est $0{,}3 \leqq P_{He}$ (torr) $\leqq 5$ pour la pression d'hélium $10^9 \leqq n_e(\text{cm}^{-3}) \leqq 2 \times 10^{13}\ \text{cm}^{-3}$ pour la densité électronique, $1 \leqq \varnothing\,(\text{mm}) \leqq 16$ pour le diamètre des décharges et le degré d'ionisation $\alpha \leqq 10^{-3}$. La température électronique est de l'ordre de 45 000 K.

Abstract. — A new collisional radiative model of helium capillary glow discharge has been developed that incorporates the l changing atomic collisions, the associative ionization and the n changing atomic collisions (for the states $n \geqq 8$). This model is used to determine the electron temperature of low density plasmas. The range of validity of the model is $0.3 \leqq P_{He}$ (torr) $\leqq 5$ for the helium pressure, $10^9 \leqq n_e(\text{cm}^{-3}) \leqq 2 \times 10^{13}$ for the electron density, $1 \leqq \varnothing\,(\text{mm}) \leqq 16$ for the discharge diameter and the ionisation degree $\alpha \leqslant 10^{-3}$. The electron temperature is close to 45 000 K.

1. Introduction.

In 1962, Bates *et al.* [1] introduced the collisional radiative model method for the study of hydrogen plasma in the absence of local thermodynamic equilibrium. Since then, many other works have been devoted to similar studies on different atomic systems. For example the hydrogen atomic system has been studied by Bates *et al.* [1, 2], Drawin and Emard [3] the helium system by Drawin and Emard [3, 4], Deloche [5], Hess and Burell [6], Fujimoto and Fukuda [7], Hedge *et al.* [8] and Strivastava *et al.* [9], the nitrogen system by Catherinot [10, 11], and the caesium system by Sayer *et al.* [12].

The method of the collisional radiative model (C.R.M.) consists in the resolution of a set of coupled equations (rate equations). In these equations the unknown quantities are the population densities of the levels of atoms and/or ions excited in a plasma. The rate equation coefficients are the sum of the rate coefficients of the collisional and radiative processes populating and depopulating the excited states. The values of these rate coefficients depend on the experimental conditions of the plasma. Thus, some of the plasma parameters (electron density n_e, electron temperature T_e, ...) must be known in order to get a solution of the set of equations.

The C.R.M. method can be used in the determination of the plasma parameters. In this connexion, Drawin *et al.* [13, 14] could fit experimental excited state population densities with their C.R.M. results in pure hydrogen and in pure helium glow discharges. Seemingly Catherinot [10, 11] could determine the spatial electron temperature distribution in a nitrogen plasma jet.

On the other hand, the C.R.M. method can be used in order to estimate some of the coefficients of the set of equations by direct comparison between experimental data and calculations from C.R.M. In this manner ionization and recombination coefficients in a hydrogen plasma have been calculated by Bates *et al.* [1, 2]. Similarly Deloche [5] obtained the coefficients of the most important elementary processes in a helium afterglow discharge (diffusion of atomic or molecular metastables for example).

And finally, Sayer by using a C.R.M. could study the main processes leading to a departure from local thermodynamic equilibrium (L.T.E.) in a low pressure caesium discharge.

In the present work we present a new C.R.M. for the atomic helium system in the case of a stationary discharge with a weak degree of ionization ($\alpha \leqq 10^{-3}$). The range of validity of this model is from 0.3 to 5 torr for the helium pressure P_{He}, from 300 to 400 K

for the gas temperature T_g, and from 5×10^9 to 2×10^{13} cm^{-3} for the electron density n_e. The electron temperature T_e is assumed to be in the range 30 000 K to 80 000 K. The diameter $\varnothing$ of the discharge is limited to $1 \leqq \varnothing$ (mm) $\leqq 16$.

Furthermore, the atomic collisions are taken into account as well as the electronic collisions. The originality of this work comes from the fact that the most recent experimental data are considered, in contrast to the recent work done by Hedge and Ghosh [8] and Strivastava *et al.* [9]. These authors used the theoretical atomic cross sections proposed by Drawin *et al.* [15] which were inferred from associative ionization coefficients given by Drawin [16] for the helium system. Here, we prefer to use recent experimental data given by Dubreuil and/or Catherinot [17-19], Gauthier *et al.* [20] for the atomic L-changing collisions and associative ionization and the ones given by Devos *et al.* [21] for atomic n-changing collisions.

The present C.R.M. is used to estimate the electron temperature which is otherwise very difficult to determine in a capillary glow discharge. Two methods are applied. The temperature is first obtained by comparison between the measured population densities and those calculated from our model and secondly by the solution of the electron rate equations without comparison with experimental data.

In section 2, we present our C.R.M. and the basic hypothesis. In section 3, we discuss the choice of the atomic data used in our model. They have been selected from all the data presently available. In section 4, the numerical method of resolution of the set of rate equations is given. In section 5, we describe computations of the electron temperature in a glow discharge (4 mm in diameter) at two pressures (1 and 4.5 torr) for the same current. Then, also in section 5 a comparison between the results of our model and the experiment of Fujimoto [7] is made and finally we give a conclusion in section 6.

2. Description of the model.

2.1 ELEMENTARY PROCESSES. — In this C.R.M., it is assumed that the only processes producing transitions between the energy levels of the atom are spontaneous radiative decay, electron collisions and atom collisions. These reactions can be written respectively :

---

react. I

$$\mathrm{He} \mid n, L, S \rangle \xrightarrow{A[\mid n, L, S \rangle ; \mid n', L \pm 1, S \rangle]} \mathrm{He} \mid n', L \pm 1, S \rangle + h\nu$$

for the radiative transitions;

react. II

$$\mathrm{He} \mid n, L, S \rangle + \mathrm{e}^- \underset{k[\mid n', L', S' \rangle ; \mid n, L, S \rangle]}{\overset{k[\mid n, L, S \rangle ; \mid n', L', S' \rangle]}{\rightleftharpoons}} \mathrm{He} \mid n', L', S' \rangle + \mathrm{e}^-$$

for the excitation transfers by electronic collisions;

react. IIIa

$$\mathrm{He} \mid n, L, S \rangle + \mathrm{He} \mid 1\,{}^1\mathrm{S} \rangle \underset{k^N[\mid n, L', S \rangle ; \mid n, L, S \rangle]}{\overset{k^N[\mid n, L, S \rangle ; \mid n, L', S \rangle]}{\rightleftharpoons}} \mathrm{He} \mid n, L', S \rangle + \mathrm{He} \mid 1\,{}^1\mathrm{S} \rangle$$

for the atomic L changing collisions;

react. IIIb

$$\mathrm{He} \mid n, L, S \rangle + \mathrm{He} \mid 1\,{}^1\mathrm{S} \rangle \underset{k^N[\mid n', L', S \rangle ; \mid n, L, S \rangle]}{\overset{k^N[\mid n, L, S \rangle ; \mid n', L', S \rangle]}{\rightleftharpoons}} \mathrm{He} \mid n', L', S \rangle + \mathrm{He} \mid 1\,{}^1\mathrm{S} \rangle$$

for the atomic n changing collisions.

The symbols above and below the arrows represent the rate coefficients as they will be used throughout this paper :

In the reactions, n, L, S are respectively the principal, orbital and spin quantum numbers of the initial state. The prime refers to the final state if the quantum numbers are changed during the reaction. In reaction III, $\mid 1\,{}^1\mathrm{S} \rangle$ denotes the ground state of the helium atom.

Other processes included in the model are ionization of the atom from any of the levels due to electronic collisions and associative ionization :

react. IV

$$\mathrm{He} \mid n, L, S \rangle + \mathrm{e}^- \xrightarrow{S[\mid n, L, S \rangle]} \mathrm{He}^+ + \mathrm{e}^- + \mathrm{e}^-$$

react. V

$$\mathrm{He} \mid n, L, S \rangle + \mathrm{He} \mid 1\,{}^1\mathrm{S} \rangle \xrightarrow{S^N[\mid n, L, S \rangle]} \mathrm{He}_2^+ + \mathrm{e}^- .$$

Inelastic collisions involving two metastable atoms that have large populations, must be included. The corresponding processes are give by Biondi [22] for helium:

react. VIa

$$\mathrm{He} \mid 2\,{}^3\mathrm{S} \rangle + \mathrm{He} \mid 2\,{}^3\mathrm{S} \rangle \xrightarrow{h(1)} \mathrm{He}^+ + \mathrm{He} + \mathrm{e}^- \longrightarrow \mathrm{He}_2^+ + \mathrm{e}^-$$

react. VIb

$$\mathrm{He} \mid 2\,{}^3\mathrm{S} \rangle + \mathrm{He} \mid 2\,{}^1\mathrm{S} \rangle \xrightarrow{h(2)} \mathrm{He}^+ + \mathrm{He} + \mathrm{e}^- \longrightarrow \mathrm{He}_2^+ + \mathrm{e}^-$$

react. VIc

$$\mathrm{He} \mid 2\,{}^1\mathrm{S} \rangle + \mathrm{He} \mid 2\,{}^1\mathrm{S} \rangle \xrightarrow{h(3)} \mathrm{He}^+ + \mathrm{He} + \mathrm{e}^- \longrightarrow \mathrm{He}_2^+ + \mathrm{e}^- .$$

Reciprocally, the three body recombination and the radiative recombinaison processes could be included in the model but they were negligible as shown in section II.5. The corresponding reactions are :

react. VIIa

$$\mathrm{He}^+ + \mathrm{e}^- + \mathrm{e}^- \xrightarrow{R[\mid n, L, S \rangle]} \mathrm{He} \mid n, L, S \rangle + \mathrm{e}^-$$

react. VIIb

$$\mathrm{He}^+ + \mathrm{e}^- \xrightarrow{\beta[\mid n, L, S \rangle]} \mathrm{He} \mid n, L, S \rangle + h\nu .$$

Moreover, the inverse process of reaction V, namely dissociative recombination (leaving the atom in an excited state), becomes important only at higher neutral densities than the ones considered here. It was therefore neglected in the present model.

Dielectronic recombination caused by electron capture into the autoionizing states may have some effect on the population densities, but according to Drawin [4] this effect is small except for electron densities lower than 10^{12} cm^{-3} and electron temperature larger than 10 eV which is not the case here.

On the other hand excited states of the He^+ ion are neglected. All He^+ ions are considered to be in the ground state. Moreover, according to Deloche and references therein [74] the density of the molecular ions He_2^+ is very small compared to the density of the He^+ ions in the working pressure range. Consequently every process involving the He_2^+ ions is neglected in our model.

Finally, a conversion mechanism of triplet metastable atoms into metastable molecules by collisions with two atoms in the ground state was proposed by Phelps [23] following the reaction

react. VIII

$$\mathrm{He} \mid 2\,{}^3\mathrm{S} \rangle + 2\,\mathrm{He} \mid 2\,{}^1\mathrm{S} \rangle \rightarrow \mathrm{He}_2 \mid 2\,{}^3\mathrm{S}\Sigma_u^+ \rangle + \mathrm{He} \mid 1\,{}^1\mathrm{S} \rangle .$$

But at the operating pressure considered here, this process can be neglected according to Deloche [5]. On the contrary, the process of metastable diffusion to the wall is the most important process of metastable losses and must be considered in the model.

2.2 RATE EQUATIONS. — In the following, p and q represent the $|\, n, L, S \,\rangle$ and $|\, n', L', S' \,|$ excited states ordered with increasing energy.

For an excited level p having a population density $n(p)$ the rate equation can be written as

$$\left.\begin{aligned}\frac{dn(p)}{dt} = &\sum_{q\neq p} k(q,p)\, n_e\, n(q) + \sum_{q>p} A(q,p)\, n(q) - \sum_{q\neq p} k(p,q)\, n_e\, n(p) - \\ &- \sum_{q<p} A(p,q)\, n(p) - S(p)\, n_e\, n(p) + R(p)\, n_e^2\, n_i + \beta(p)\, n_e\, n_i \\ &- \sum_{q\neq p} k^N(p,q)\, n(p)\, n(1\ ^1S) + \sum_{q\neq p} k^N(q,p)\, n(q)\, n(1\ ^1S) \\ &- S^N(p)\, n(p)\, n(1\ ^1S)\end{aligned}\right\} \quad (1)$$

where the notation of section 2.1 is used, and where n_i is the ion density. Assuming $n(He_2^+) \ll n_e$, the condition for electrical neutrality in the plasma yields $n_e = n_i$. By hypothesis the ratio $n_e/n(1\ ^1S)$ is smaller than 10^{-3} and the gas temperature is assumed to be constant across the discharge radius. From these assumptions $n(1\ ^1S)$ obeys the ideal gas equation

$$P_{He} = n(1\ ^1S)\, kT_g \quad (2)$$

where T_g is the gas temperature.

Consequently, it is not necessary to solve the $1\ ^1S$ rate equation and $n(1\ ^1S)$ is considered as a parameter.

The left hand side of equation (1) can be expressed by the relation

$$\frac{dn(p)}{dt} \cong \frac{\partial n(p)}{\partial t} + \frac{D(p)}{\delta^2}\, n(p) \quad (3)$$

with $\delta = R/2.4$, R being the discharge radius and $D(p)$ being the diffusion coefficient of the He atom in the state p. Because only stationary discharges are studied here we can write $\partial n(p)/\partial t = 0$ for any p.

The collisional lifetime of non-metastable states is much smaller than their diffusion time. Thus, we can put $D(p) = 0$ for every p which does not refer to the metastable levels.

The normalized population density (or the Saha decrement) ρ is defined by

$$\rho(p) = n(p)/n^E(p) \quad (4)$$

where $n^E(p)$ is given by the Saha Boltzmann law.

Application of the microreversibility relations gives :

$$k(q,p) = \frac{n^E(p)}{n^E(q)}\, k(p,q) \qquad \text{for} \qquad p < q \quad (5a)$$

and

$$R(p) = \frac{n^E(p)}{n_e^2}\, S(p)\,. \quad (5b)$$

When these equations and equation (3) are put into equation (1) the M equations with M unknown quantities become :

$$b(p) = \sum_{q=1}^{M} a(p,q)\, \rho(q) \qquad \text{for any} \qquad p \neq |\, 1\ ^1S \,\rangle \quad (6)$$

where (with the exception of He metastable levels $2\ ^1S$, $2\ ^3S$) :

$$b(p) = -\, n_e[S(p)\, n^E(p) + \beta(p)\, n_e + k(1\ ^1S, p)\, n(1\ ^1S)] \quad (7a)$$

$$a(p,q) = k(p,q)\, n^E(p)\, n_e + A(q,p)\, n^E(q) + k^N(q,p)\, n^E(q)\, n(1\ ^1S) \quad \text{for} \quad p < q \quad (7b)$$

$$\begin{aligned}a(p,q) = &-\, [S(p)\, n_e + S^N(p)\, n(1\ ^1S)]\, n^E(p) - \sum_{i=p+1}^{M} k(p,i)\, n_e\, n^E(p) \\ &- \sum_{i=1}^{p-1} k(i,p)\, n_e\, n^E(i) - \sum_{i=1}^{p-1} A(p,i)\, n^E(p) \\ &- \sum_{j\neq p} k^N(p,j)\, n(1\ ^1S)\, n^E(p) \qquad \text{for} \qquad p = q\end{aligned} \quad (7c)$$

$$a(p,q) = k(q,p)\, n^E(q)\, n_e + k^N(q,p)\, n^E(q)\, n(1\ ^1S) \qquad \text{for} \qquad p > q\,. \quad (7d)$$

Furthermore, non-linear processes due to collisions between 2 ^{1}S or/and 2 ^{3}S atoms may be important in the destruction of the atomic metastable levels and they must be included in the framework of our formulation (Eq. (6)) by the addition of appropriate terms on the right-hand side of (7*c*). In these equations the diffusion terms of metastable atoms are also included. Hence, with $p = 1$ and $p = 2$ representing the states 2 ^{3}S and 2 ^{1}S respectively, the coefficient $a(1, 1)$ for the 2 ^{3}S level becomes :

$$a'(1, 1) = a(1, 1) - d(1)\, n^E(1)\, n^2(1\,\mathrm{S}) - h(1)\, n^E(1)\, n^E(1)\, \rho(1) - h(2)\, n^E(1)\, n^E(2)\, \rho(2) - \frac{D(1)}{\delta^2}\, n^E(1) \qquad (7c')$$

and for the 2 ^{1}S level we get

$$a'(2, 2) = a(2, 2) - h(2)\, n^E(1)\, n^E(2)\, \rho(1) - h(3)\, n^E(r)\, n^E(2)\, \rho(2) - \frac{D(2)}{\delta^2}\, n^E(2) \qquad (7c'')$$

with $a(p, p)$ from (7*c*).

Finally, for all line transitions terminating in the ground state, the effect of radiation trapping is considered, by introducing the escape factor Λ first defined by Holstein [24] and re-investigated recently by Irons [25].

The transition probability is therefore written as

$$\Lambda(p, 1\,^1\mathrm{S}) \times A(p, 1\,^1\mathrm{S}) \quad \text{with} \quad 0 \leqq \Lambda(p, 1\,^1\mathrm{S}) \leqq 1\,.$$

This coefficient has been calculated by Drawin and Emard [26] for Doppler and natural line broadenings.

We also consider the radiation trapping effect for lines terminating on the metastable states. This effect introduces some new non-linear terms in equation (6) because the escape factors depend on the metastable population densities.

2.3 GENERAL CONSIDERATIONS FOR ATOMIC COLLISIONS. — According to Hess [6], Fujimoto [7], Dubreuil [17] and Catherinot [18], in helium, the non-degeneracy of singlet and triplet levels and of the angular momentum sublevels of a particular principal quantum number means that the population of these sublevels will not be in statistical equilibrium under many plasma conditions.

But for two sublevels, with an energy gap ΔE smaller than the mean kinetic energy kT_g of the heavy particules, the departure from statistical equilibrium is reduced by L-changing collisions (reaction IIIa).

This effect increases with n, since ΔE decreases and because the coefficient of reaction IIIa increases when ΔE decreases. This behaviour of L-changing cross sections in shown in figure 1 taken from the paper of Catherinot and Dubreuil [18]. In this figure, the thermally averaged cross sections for the excitation transfer $\sigma_{ij} = k^N(i, j)/\langle v_{He} \rangle$ are reported as a function of the dimensionless ratio $\Delta E_{ij}/kT_g$.

Thus, for $n \geqq 8$ the excitation transfers by atomic L-changing collisions are much faster than any other process (spontaneous radiative transition, electronic collisions, ...). For example, at $p_{He} = 1$ torr, $n_e = 10^{11}$ cm^{-3} and $T_e \cong 54\,000$ K, the L-changing collision frequency for the transition from the 8 ^{3}S level to the 8 ^{3}F level is close to 10^8 s^{-1} while the frequencies of excitation transfer by electronic and atomic collisions from the $n = 8$ level to $n = 9$ level are respectively 2×10^6 s^{-1} and 10^6 s^{-1}. Consequently, the sublevel populations for $n \geqq 8$ can be considered to be in statistical equilibrium for our working pressure : $0.3 \leqq P_{He}$ (torr) $\leqq 5$. Therefore, there is no interest in considering individual $| n, L, S \rangle$ states for $n \geqq 8$ and the reactions II and IIIb, for example, can be simply taken into account as the excitation transfers between hydrogenic $| n \rangle$ and $| n' \rangle$ Rydberg levels :

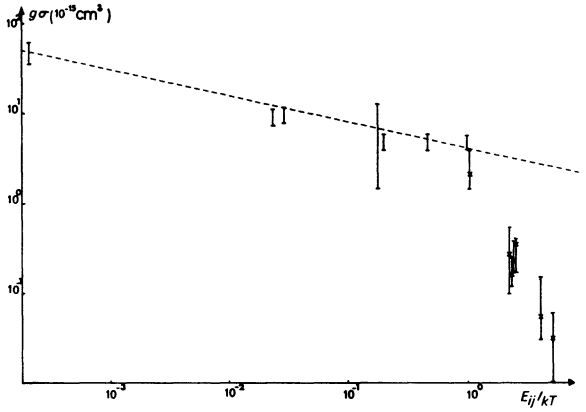

Fig. 1. — Thermally averaged cross sections for excitation transfer as a function of the dimensionless ratio E_{ij}/kT_g, with E_{ij} = energy difference. I experimental values taken from papers [17-19], ------- calculated values with (9*a*), × calculated values with (9*b*).

react. II'

$$\mathrm{He} \mid n \rangle + \mathrm{e}^- \leftrightarrows \mathrm{He} \mid n' \rangle + \mathrm{e}^-$$

react. IIIb'

$$\mathrm{He} \mid n \rangle + \mathrm{He} \mid 1\,^1\mathrm{S} \rangle \leftrightarrows \mathrm{He} \mid n' \rangle + \mathrm{He} \mid 1\,^1\mathrm{S} \rangle\,.$$

Furthermore, according to the Wigner spin conser-

vation rules, the contributions of reactions like

$$\mathrm{He} \mid n, L < 3, S \rangle + \mathrm{He} \mid 1\ ^1\mathrm{S} \rangle \rightleftarrows \rightleftarrows \mathrm{He} \mid n, L' < 3, S' \rangle + \mathrm{He} \mid 1\ ^1\mathrm{S} \rangle$$

with $S \neq S'$
are negligible and in this case we can put $K^N(n, L < 3, S; n, L' < 3, S') = 0$ in equation (6) as long as $L \geqq 3$. For these levels the spin is not a good quantum number according to Van den Eynde *et al.* [27], Abrams and Volga [28]. These groups of sublevels play an important part in singlet-triplet excitation transfers by atomic collisions as shown by Catherinot and Dubreuil [18].

Thus, the coefficients $K^N(p, q)$ are put equal to zero when p and q are related to sublevels with different spin numbers except for the level ^{1,3}F, ^{1,3}G. The $K^N(p, q)$ are also put equal to zero, when p and q connect levels with different principal quantum numbers smaller than 8, the energy gap between these levels being larger than kT_g,

2.4 GENERAL CONSIDERATIONS FOR ELECTRONIC COLLISIONS. — According to Fujimoto [7] the low-lying levels ($n \leqq 7$) are populated mainly by electronic collisions from the ground state and, secondly, from 2 ^{1,3}S metastable states. Fujimoto [7] following Johnson and Hinnov [29] supposes that an $\mid n \rangle$ level with $n > 7$ is predominatly populated by excitation from the adjacent lower $\mid n - 1 \rangle$ and depopulated by excitation to the adjacent higher level $\mid n+1 \rangle$. But, as recently observed by Devos *et al.* [21], the frequencies of excitation transfer by electronic and atomic collisions from an $\mid n - 1 \rangle$ level to an $\mid n \rangle$ level ($n > 7$) are the same order of magnitude (see the example given in section 2.3).

On the other hand, it follows from the results of Catherinot and Dubreuil [17, 18] that the electronic L-changing collisions for $n \leqq 7$ are inefficient in our experimental conditions. Moreover, these authors demonstrated experimentally that the electronic n-changing collisions (with $n = 3, 4, 5$) are also inefficient at $n_e \leqq 10^{11}$ cm^{-3}. But at larger n_e, namely $n_e \cong 1.5 \times 10^{13}$ cm^{-3}, the rates of excitation transfer by electronic collisions between the n levels ($n = 5$, 6, 7 and 8) can be larger than the spontaneous radiative decay (for example $n_e\, k\,(n = 6, n = 5) = 6.7 \pm 3.9 \times 10^7$ s^{-1} and $A(6, 5) = 10^6$ s^{-1} at $n_e \cong 1.5 \times 10^{13}$ cm^{-3}) as shown in a recent experiment (G. Gousset *et al.* [30]).

Thus, for a correct description in the electron density range $n_e = 5 \times 10^9$ to 2×10^{13} cm^{-3}, electronic n-changing collisions between the levels $3 \leqq n \leqq 8$ must be considered.

In the process of n-changing collisions, the allowed transitions $n\ ^{1,3}L \rightarrow m\ ^{1,3}(L \pm 1)$ are assumed to be predominant. Consequently we put in (6) $k(p, q) = 0$ if p and q refer to two levels ($3 \leqq n \leqq 7$) with different spin quantum number or with $L - L' \neq \pm 1$.

2.5 REMARK ON THE ELECTRON-ION RECOMBINATION. — The left hand side $b(p)$ of (6) contains the contribution of the radiative and three-body recombination to the population of a level $\mid p \rangle$. The third term represents the electronic excitation rate of the $\mid p \rangle$ level from the ground state. Under our experimental conditions ($T_e > 30\,000$ K, $10^9 \leqq n_e$ [cm^{-3}] $\leqq 2 \times 10^{13}$ and $\alpha < 10^{-3}$) the first terms are very small compared to this third term. For instance, at $P_{He} = 1$ torr ($n(1\ ^1\mathrm{S}) \cong 3 \times 10^{16}$ cm^{-3}), $T_e = 54\,000$ K and $n_e = 10^{11}$ cm^{-3}, for the level 2 ^{1}P we get $n_e^2\, \beta(\mathrm{p}) \cong 3.\ 10^7$ cm^{-3} s^{-1} from Gingerich [31], $n_e\, S(2\ ^1\mathrm{P})\, n^E(2\ ^1\mathrm{P}) = n_e^3\, R(2\ ^1\mathrm{P}) = 3 \times 10^4$ cm^{-3} s^{-1} and $n_e\, k(1\ ^1\mathrm{S}, 2\ ^1\mathrm{P}) = 2 \times 10^{16}$ cm^{-3} s^{-1} from Drawin [32]. As expected, the coefficient $\beta(p)$ decreases when the excitation energy $E(p)$ of the p level increases. Though the coefficient of three-body recombination increases with $E(p)$, the recombination rate remains smaller than the third term of (7*a*), except for very high levels $n \geqq 30$, not considered here.

Thus the radiative and three-body recombination have been neglected here.

3. Atomic parameters.

3.1 RADIATIVE COEFFICIENTS. — The transition probabilities are inferred from oscillator strengths calculated by Dubreuil and Chapelle [33] using the quantum defect method (Bates and Daamgard [34]).

3.2 INELASTIC ELECTRONIC CROSS SECTIONS. — Many experimental and theoretical data are reported for cross sections of electronic excitation from ground and metastable levels. On the contrary only one paper by Burell and Kunze [35], could be found for levels $3 \leqq n \leqq 7$.

In our C.R.M. the semi-empirical and analytical relations of Drawin [32] for the transitions from the ground state or from the metastable states are used :

$$\sigma(p, q) = 4\,\pi a_0^2\, Q(p, q)\, [R/(E(q) - E(p))]^2 f(p, q) \times \times [(U - 1)/U] \ln [1.25\, U] \quad (8a)$$

$$\sigma(p, q) = 4\,\pi a_0^2\, Q(p, q)\, [U - 1]/U^2 \quad (8b)$$

$$\sigma(p, q) = 4\,\pi a_0^2\, Q(p, q)\, [U - 1]/U^5 \quad (8c)$$

where p denotes the states $\mid 1\ ^1\mathrm{S} \rangle$, or $\mid 2\ ^3\mathrm{S} \rangle$, or $\mid 2\ ^1\mathrm{S} \rangle$. If $p \equiv \mid 1\ ^1\mathrm{S} \rangle$ (8*a*) refers to the transitions $1\ ^1\mathrm{S} \rightarrow \mathrm{n}\ ^1\mathrm{P}$, (8*b*) to the transitions $1\ ^1\mathrm{S} \rightarrow n\ ^1L (L \neq P)$ and (8*c*) to the transition $1\ ^1\mathrm{S} \rightarrow n\ ^3L$. In these formulae, a_0 is the Bohr radius in cm, $E(q)$ is the excitation potential of the level $\mid q \rangle$ in cm^{-1} and $U = E/E(q)$, where E is the free electron energy. R is the Rydberg energy in cm^{-1} and $f(1\ ^1\mathrm{S}, q)$ is the absorption oscillator strength of the transition. Finally, $Q(1\ ^1\mathrm{S}, q)$ are adjustable parameters determined by experiment and/or theoretical data.

For the $1\ ^1\mathrm{S} \rightarrow n\ ^1\mathrm{P}$ transitions (8*a*) was fitted to the values given by St John *et al.* [36], Jobe and

St John [37], Moustafa Moussa *et al.* [38], Van Raan *et al.* [39], Hall *et al.* [40], Mc Cann and Flannery [41], Scott and McDowell [42], Strivastava and Rai [43], Baluja and McDowell [44], Bhadra *et al.* [45], Wersterveld *et al.* [46], Fon *et al.* [47] and Vriens *et al.* [48].

The cross section for $1\ ^1S - n\ ^1L$ ($L \neq P$) transitions are fitted by (8*b*) using the cross section values of St John *et al.* [36], Van Raan *et al.* [39, 49], Hall *et al.* 40], Bhadra *et al.* [45], Trajmar [50], Ton That *et al.* [51], Roy and Syl [52], Fon *et al.* [53].

For the $1\ ^1S - n\ ^3L$ transitions we use the data given by St John *et al.* [36], Jobe and St John [37], Baluja and McDowell [44], Bhadra *et al.* [45], Ton That *et al.* [51], Van Raan *et al.* [49], Fon *et al.* [54] and Hall *et al.* [40].

The coefficients $Q(1\ ^1S, p)$ become proportional to n^{*-3} for $n \geqq 7$, n^* being the effective quantum number of the upper level of the transition. In this case the coefficients of Drawin [32] are used.

When $p \equiv |\, 2\ ^3S\,\rangle$ or $p \equiv |\, 2\ ^1S\,\rangle$, for the transitions with no multiplicity change : $2\ ^{1,3}S \rightarrow n\ ^{1,3}P$ and $2\ ^{1,3}S \rightarrow n\ ^{1,3}L \neq P$, $Q(2\ ^{1,3}S, q)$ is determined by comparison of the values given by (8*a*) and (8*b*) and the data given by Flannery and McCann [55], Ochkur and Bratsev [56] and Khayrallah *et al.* [57].

For the $2\ ^{1,3}S - n\ ^{1,3}L$ transitions with a change in multiplicity, Drawin [32] suggested using the empirical relation

$$q_{ij} = 4\,\pi a_0^2\, Q U^{-1}$$

but there was no confirmation of this behaviour.

We suggest keeping the same cross section given by (8*c*). With the correct Q, this form fits accurately the cross section values given by Ochkur and Bratsev [56] and Mariott [58] over a large range of electron kinetic energy.

Two examples of fits are shown in figure 2*a* for the transition $1\ ^1S \rightarrow 2\ ^1P$ and in figure 2*b* for the transition $1\ ^1S \rightarrow 3\ ^1P$.

For the transitions $n\ ^{1,3}L \rightarrow m\ ^{1,3}(L \pm 1)$ no experimental data exist other than the work of Burell and Kunze [35]; in this case we could use two different semi-empirical hydrogenic formulae given either by Johnson [59] or by Vriens and Smeets [60].

The Vriens and Smeets theoretical cross sections are in good agreement with the measurements by Devos *et al.* [21] for the levels $n \geqq 8$ at a low electron temperature $T_e \cong 3\,000$ K.

For electron temperatures ranging from 30 000 K to 60 000 K as in our experimental conditions, the Vriens form disagrees with the analytic form given by Johnson by three orders of magnitude. However, a recent experiment using an infrared laser perturbation in a capillary glow discharge at low pressure (G. Gousset *et al.* [30]) shows that cross sections given by Johnson has the correct order of magnitude. Hence they were choosen for our model calculation.

For the ionization cross section, the Drawin formulae have been used.

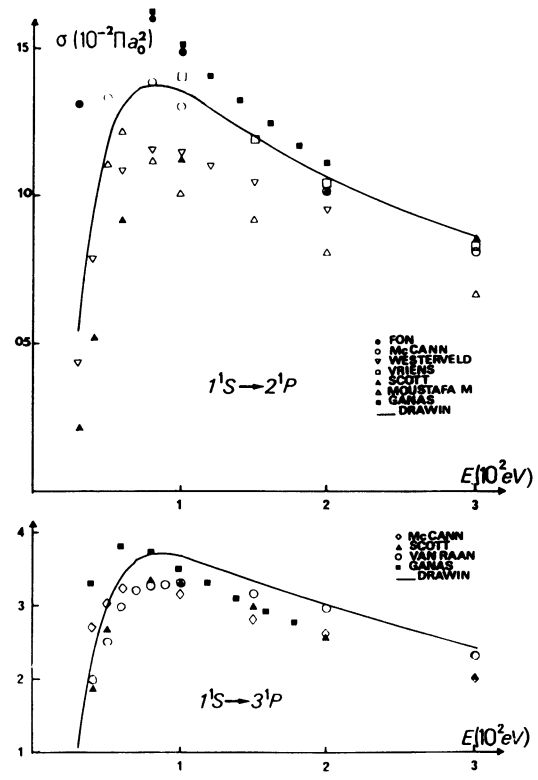

Fig. 2. — Cross sections for electronic collisions of allowed transitions from ground state as a function of electron kinetic energy.

a) Transition $1\ ^1S \rightarrow 2\ ^1P$, ——— Calculated curve from (8*a*) with $Q(1\ ^1S, 2\ ^1P) = 1$. Experimental and/or theoretical data : ● Ref. [47], ○ Ref. [41], ▽ Ref. [46], □ Ref. [48], ▲ Ref. [43], △ Ref. [38].

b) Transition $1\ ^1S \rightarrow 3\ ^1P$. ——— Calculated curve from (8*a*) with $Q(1\ S, 3\ P) = 1.2$. Experimental and/or theoretical data : ◇ Ref. [41], △ Ref. [42], ○ Ref. [39].

3.3 INELASTIC ELECTRONIC RATE COEFFICIENTS. — Integration of the electronic cross sections over a Maxwellian electron energy distribution yielded rate coefficients that could be expressed in terms of exponential integrals or in terms of a function ψ tabuled by Drawin [32].

Effectively according to Allis [62] when the ratio E/P_{He} of the electric field strength to the pressure is larger than 4.9 $eV/cm^{-1}\ torr^{-1}$, the distribution function of the electrons fluctuates around a Maxwell distribution function having the same average energy.

Hence it is probably correct to suppose that the error in the calculation of the electronic coefficient rates for ionization and excitation is negligible when the electronic cross sections used in our model are integrated over the Maxwell energy distribution function instead of the Allis function.

3.4 INELASTIC ATOMIC RATE COEFFICIENTS. — The rate coefficients of L changing collisions have been reported by Gauthier *et al.* [20] and Dubreuil and Catherinot [17] for $n = 3$, Catherinot and Dubreuil [18] for $n = 4$ and the coefficients of fine structure-changing

collisions within the 3 ^{3}D state have been measured by Catherinot *et al.* [19].

The set of values is shown in figure 1 where the product $g\bar{\sigma}$ is plottend *versus* of $\Delta E/kT_g$ where $\bar{\sigma} = k^N(p, q)/\langle v \rangle$ and g_p is the statistical weight of the starting level of the transition.

We suggest using the following empirical analytical formulae to fit the experimental values given in figure 1 :

$$K^N(p, q) = 7.76 \times 10^{-10}\left[\frac{E(p, q)}{KT_g}\right]^{-0.29} \frac{1}{g(p)} \quad \text{if } p < q \quad (9a)$$

for $E(p, q)/kT_g < 1$ and

$$K^N(p, q) = 7.76 \times 10^{-10}\left[\frac{E(p, q)}{kT_g}\right]^{-0.29} \frac{1}{g(p)} \times \times e^{-aE(p,q)/kT_g} \quad (9b)$$

for $p < q$ and $E(p, q)/kT_g > 1$.

In the last equation, the parameter a is close to unity and depends slightly on the transition $p \rightarrow q$.

This analytical expression simplifies the model calculations and allows us to extrapolate the L changing collision rate coefficients for $n = 5$, 6 and 7.

For rate coefficients of excitation transfers between two $n \geqq 8$ levels, the analytical formula given by Devos *et al.* [21] has been used.

For associative ionization rate coefficients, an analytical form cannot be worked out, thus, in order to extrapolate the experimental values given for $n=3$ and 4 by Dubreuil and/or Catherinot [17-20], to $n \geqq 5$ we suppose that the rate coefficients do not vary too rapidly with n. This assumption has been recently confirmed by measurements for $n = 5$ (Dubreuil and Catherinot [63] and Pennel [64]).

Table I. — *Energy levels considered in our model.*

n	Nomination	Energy [cm^{-1}]	L	S	G
1	1^1S	0	0	0	1
2	2^3S	159 856 . 069	0	1	3
2	2^1S	166 277 . 547	0	0	1
2	2^3P	169 087 . 24	1	1	9
2	2^1P	171 135 . 00	1	0	3
3	3^3S	183 236 . 892	0	1	3
3	3^1S	184 864 . 936	0	0	1
3	3^3P	185 564 . 759	1	1	9
3	3^3D	186 101 . 66	2	1	15
3	3^1D	186 105 . 065	2	0	5
3	3^1P	186 209 . 471	1	0	3
4	4^3S	190 298 . 21	0	1	3
4	4^1S	190 940 . 331	0	0	1
4	4^3P	191 217 . 14	1	1	9
4	4^3D	191 444 . 591	2	1	15
4	4^1D	191 446 . 559	2	0	5
4	$4^3,^1F$	191 451 . 94	3	0 et 1	28
4	4^1P	191 492 . 817	1	0	3
5	5^3S	193 347 . 089	0	1	3
5	5^1S	193 663 . 627	0	0	1
5	5^3P	193 800 . 78	1	1	9
5	5^3D	193 917 . 245	2	1	15
5	5^1D	193 918 . 391	2	0	5
5	$5^3,^1F,G$	193 921 . 73	3.4	0 et 1	64
5	5^1P	193 942 . 57	1	0	3
6	6^3S	194 936 . 23	0	1	3
6	6^1S	195 115 . 00	0	0	1
6	6^3P	195 192 . 91	1	1	9
6	6^3D	195 260 . 167	2	1	15
6	6^1D	195 260 . 86	2	0	5
6	$6^3,^1F,G,H$	195 263 . 20	3.4.5	0 et 1	108
6	6^1P	195 275 . 04	1	0	3
7	7^3S	195 868 . 35	0	1	3
7	7^1S	195 979 . 04	0	0	1
7	7^3P	196 027 . 40	1	1	9
7	7^3D	196 069 . 73	2	1	15
7	7^1D	196 070 . 16	2	0	5
7	$7^3,^1F,G,H,I$	196 071 . 74	3.4.5.6	0 et 1	160
7	7^1P	196 079 . 24	1	0	3
8	8	196 568 . 46			256
9	9	196 936 . 66			324
10	10	197 197 . 34			400
11	11	197 391 . 86			484
12	12	197 539 . 49			576
13	13	197 654 . 23			676
14	14	197 744 . 18			784
15	15	197 818 . 4			900
16	16	197 878 . 28			1024
17	17	197 927 . 88			1156
18	18	197 971 . 60			1296
19	19	198 006 . 27			1444
20	20	198 036 . 13			1600

3.5 OTHER DATA. — These data concern the processes related to the metastable atoms.

The symbols $h(1)$, $h(2)$ and $h(3)$ denote the ionization rate coefficients of the 2 ^{1}S and 2 ^{3}S states due to metastable-metastable collisions (reactions VI). The values of these coefficients were taken from Johnson and Gerardo [65]. The values of the rate coefficient of depopulation of metastable atoms due to three body collisions, $d(1)$, (reaction VIII), were taken from Phelps [23]. The values of the diffusion coefficients of 2 ^{1,3}S atoms, $D(1)$ and $D(2)$, have been given by Deloche for $T_g = 293$ K. The effect of the gas temperature is considered in our model following Morgan and Schiff [66], i.e. : the product of the diffusion coefficient by the pressure is proportional to $T_g^{3/2}$.

Finally, in table I we give the energy of the levels (Martins [67]) considered in our model.

4. Solution of the set of M equations with M unknown quantities.

In our case, in addition to the various coefficients intervening in the set of equations, five plasma parameters must be known in order to get a solution : the electron density, the gas temperature, the neutral density, the discharge diameter and the electron temperature. The four first parameters can be found experimentally but the electron temperature is precisely the quantity that we try to estimate by using the model. The estimation of the electron temperature is performed following the method of Drawin *et al.* [13]. The constants of the M coupled equations are calculated with the four experimental parameters and with a starting electron temperature close to 45 000 K deduced from physical reasoning (Allis [62]). Then, the set of M equations is solved and the population densities so calculated are compared with the experimental data. Difficulties arise from the fact that extremely large differences are observed among the calculated constants and that some equations are non-linear. Thus, two iterative algorithms are necessary to solve the system and to get the population density of excited states, i.e. : the solution of the non linear system by the Newton-Raphson algorithm and the solution of linear equation by the Gauss-Seidel method [68].

5. Results and discussions.

5.1 COMPARISON OF THE C.R.M. WITH OUR EXPERIMENTS. — In section 4, we mentioned that the C.R.M. method of Drawin [13] was used to determine the electron temperature of a plasma. Using this method

the measured population densities of excited states are compared with those calculated by our C.R.M. for some electron temperature values and for fixed values of the other parameters (n_e, T_g, $\varnothing$, $N(1\ ^1S)$). Our experimental set-up is quite similar to the one previously used by Catherinot and Dubreuil [17-19]. The population densities of sublevels $|\ n, L, S\ \rangle$ ($3 \leqq n \leqq 7$) at $P_{He} = 1$ torr, then $P_{He} = 4.5$ torr, at a current of 50 mA in a $\varnothing = 4$ mm diameter and a 4 cm length tube, have been measured as absolute values by a standard method of emission spectroscopy. The $2\ ^3S$ and $2\ ^3P$ population densities have been determined from the absorption measurement of a tunable dye laser beam. The dye laser excited by a nitrogen laser was tuned on the wavelengths of the $2\ ^3S \rightarrow 3\ ^3P$ or the $2\ ^3P \rightarrow 2\ ^3D$ transitions. The corresponding calculation of the population densities was very similar to the one used by Mitchell and Zemansky [69].

On the other hand, the electron density has been measured using the high frequency cavity perturbation method by Dubreuil and Catherinot [17] at pressures ranging from 0.25 to 2.5 torr at current intensities I_D from 5 to 30 mA in the same discharge tube 4 mm in diameter. The electron density is proportional to the pressure and to the current intensity. Thus, the electron density values could be determined at $P_{He} = 1$ and 4.5 torr and at $I_D = 50$ mA by extrapolation from the results given in [17].

But these values as well as the values $N(1\ ^1S)$ of the ground state atom density are known to with in experimental uncertainties. Consequently, the set of equations (6) must be solved for two values of the parameters n_e and $N(1\ S)$ corresponding to the extrema ($n_{e_{max}}$, $N(1\ ^1S)_{max}$ and $n_{e_{min}}$, $N(1\ ^1S)_{min}$) of the respective ranges of uncertainty. Hence, for fixed values of the gas temperature and the discharge diameter and for various electron temperatures around the value deduced from the Allis model [62], the population densities n_p are first calculated for the pair of maximum values ($n_{e_{max}}$, $N(1\ ^1S)_{max}$) and then for the pair of minimum values ($n_{e_{min}}$, $N(1\ ^1S)_{min}$).

The Boltzmann diagrams

$$\mathrm{Log}_n \frac{n_p}{g_p} = f(1/p^*)$$

where p^* is the principal effective quantum number, are plotted for each series of sublevels $|\ L, S\ \rangle$. Thus a first set of graphs is obtained for ($n_{e_{max}}$, $N(1\ ^1S)_{max}$) for each $|\ L, S\ \rangle$ series, with the experimental points superposed. The two Boltzmann plots that obviously correspond to the same pair of values of electron temperature ($T_{e_{max}}$, $T_{e_{min}}$) and giving the best fits of these experimental data, are kept. An identical procedure was used for the values ($n_{e_{min}}$, $N(1\ ^1S)_{min}$) yielding two electron temperatures $T'_{e_{max}}$ and $T'_{e_{min}}$. Hence, the most probable temperature in the range of $T'_{e_{min}}$ and $T_{e_{max}}$. Figures 3*a*, 3*b* and 3*c* show the Boltzmann diagrams retained for each $|\ L, S\ \rangle$ series giving the best agreement with the experimental population densities at $P_{He} = 1$ torr and yielding the determination of T_e. The upper diagrams are calculated for $T_{e_{max}} = 54\,000$ K, $n_{e_{max}} = 10^{11}$ cm^{-3} and $N(1\ ^1S)_{max} = 3.3 \times 10^{16}$ cm^{-3}, and the lower ones calculated for $T'_{e_{min}} = 52\,000$ K, $n_{e_{min}} = 9 \times 10^{10}$ cm^{-3} and $N(1\ ^1S)_{min} = 2.83 \times 10^{16}$ cm^{-3}. Consequently, for $P_{He} = 1$ torr, T_e appears to range from 52 000 K to 54 000 K. The electron temperature for our experiment at $P_{He} = 4.5$ torr is determined in the same way; the values lie between 32 000 K

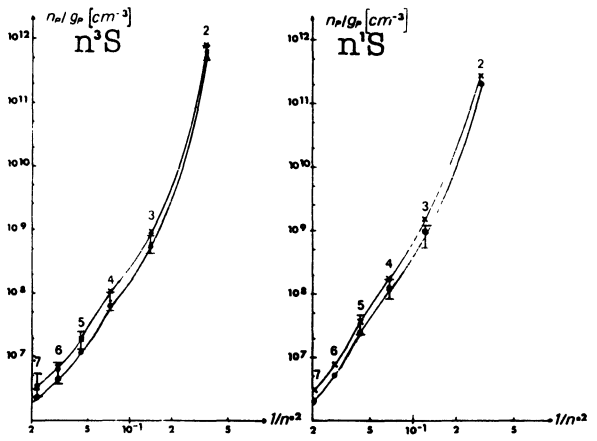

Fig. 3*a*. — Boltzmann diagrams for the levels $n\ ^3S$ and $n\ ^1S$. Comparaison between the experimental population densities (I) and the two best fits computed with our C.R.M. at 50 mA and $P_{He} = 1$ torr. The lower curve (●) corresponds to $T_e = 52\,000$ K, $n_e = 9 \times 10^{10}$ cm^{-3} and $N_1 = 2.83 \times 10^{16}$ cm^{-3} and the upper one (×) to $T_e = 54\,000$ K, $n_e = 10^{11}$ cm^{-3} and $N_1 = 3.3 \times 10^{16}$ cm^{-3}.

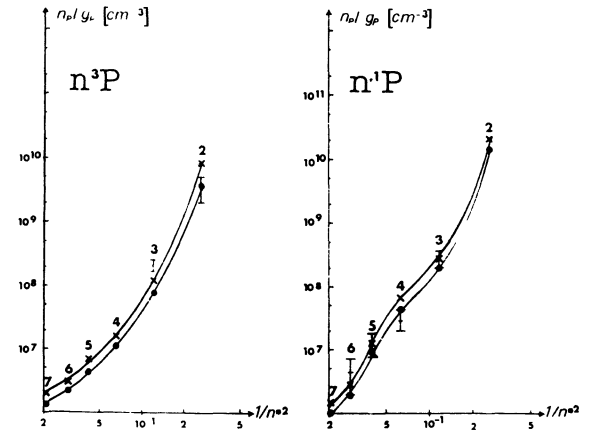

Fig. 3*b*. — Boltzmann diagrams for the levels $n\ ^3P$ and $n\ ^1P$. Comparison between the experimental population densities (I) and the two best fits computed with our C.R.M. at 50 mA and $P_{He} = 1$ torr. The lower curve (■) corresponds to $T_e = 52\,000$ K, $n_e = 9 \times 10^{10}$ cm^{-3} and $N_1 = 2.83 \times 10^{16}$ cm^{-3} and the upper one (×) to $T_e = 54\,000$ K, $n_e = 10^{11}$ cm^{-3} and $N_1 = 3.3 \times 10^{16}$ cm^{-3}.

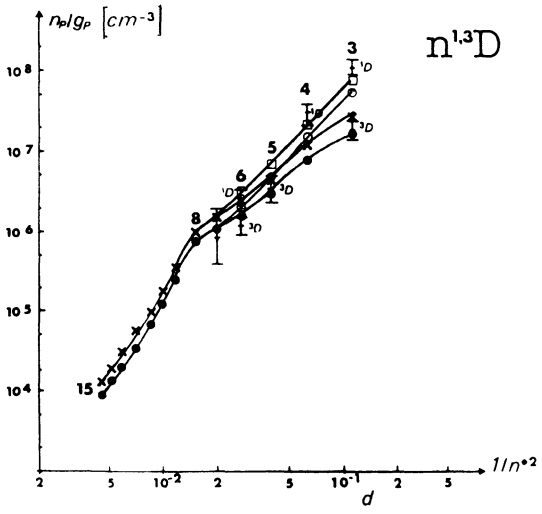

Fig. 3c. — Boltzmann diagrams for the levels $n\,^3$D and $n\,^1$D extended to $n = 20$. Comparison between the experimental population densities (I) and the best fits computed with our C.R.M. at 50 mA and $P_{He} = 1$ torr. The lower curves (○, ●) correspond to $T_e = 52\,000$ K, $n_e = 9 \times 10^{10}$ cm^{-3} and $N_1 = 2.83 \times 10^{16}$ cm^{-3} and the upper ones (□, ×) to $T_e = 54\,000$ K, $n_e = 10^{11}$ cm^{-3} and $N_1 = 3.3 \times 10^{16}$ cm^{-3}.

and 34 000 K. Figures 4*a*, 4*b* and 4*c* show the Boltzmann diagrams giving the best fit of these experimental data. Here, the upper curves are calculated for $T_{e_{max}} = 34\,000$ K, $n_{e_{max}} = 5 \times 10^{11}$ cm^{-3}, $N(1\,^1\text{S})_{max} = 1.41 \times 10^{17}$ cm^{-3}, and the lower ones for $T'_{e_{min}} = 32\,000$ K, $n_{e_{min}} = 4 \times 10^{11}$ cm^{-3}, $N(1\,\text{S})_{min} = 1.27 \times 10^{17}$ cm^{-3}.

The electron temperatures determined from our C.R.M. are close to the ones deduced by the model of Allis [62] ($T_e \cong 45\,000$ K). But neither the metastable diffusion process nor the diffusion of the charged

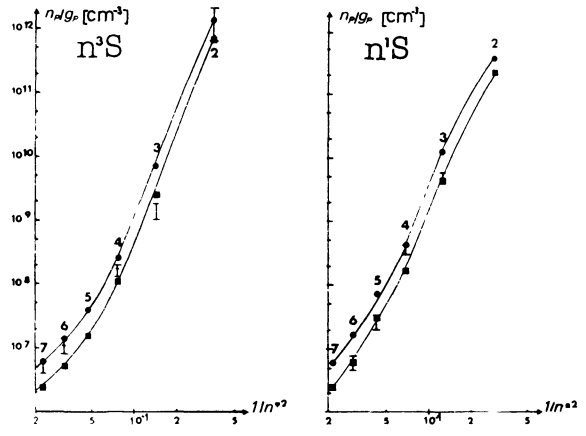

Fig. 4a. — Boltzmann diagrams for the levels $n\,^3$S and $n\,^1$S. Comparison between the experimental densities (I) and the two best fits computed with our C.R.M. at 50 mA and $P_{He} = 4.5$ torr. The lower curve (■) corresponds to $T_e = 32\,000$ K, $n_e = 4 \times 10^{11}$ cm^{-3} and $N_1 = 1.27 \times 10^{17}$ cm^{-3} and the upper one (●) to $T_e = 34\,000$ K, $n_e = 5 \times 10^{11}$ cm^{-3} and $N_1 = 1.41 \times 10^{17}$ cm^{-3}.

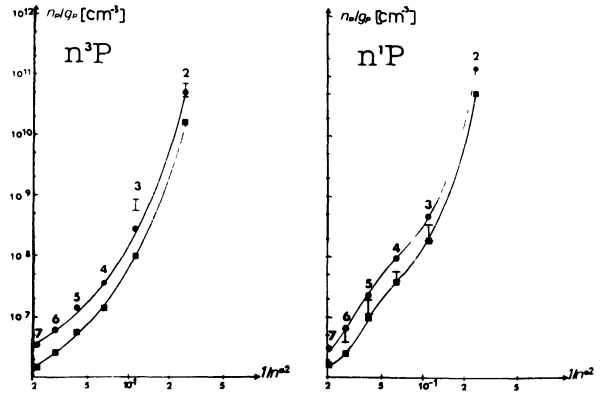

Fig. 4b. — Boltzmann diagrams for the levels $n\,^3$P and $n\,^1$P. Comparison between the experimental densities (I) and the two best fits computed with our C.R.M. at 50 mA and $P_{He} = 4.5$ torr. The lower curve (■) corresponds to $T_e = 32\,000$ K, $n_e = 4 \times 10^{11}$ cm^{-3} and $N_1 = 1.27 \times 10^{17}$ cm^{-3} and the upper one (●) to $T_e = 34\,000$ K, $n_e = 5 \times 10^{11}$ cm^{-3} and $N_1 = 1.41 \times 10^{17}$ cm^{-3}.

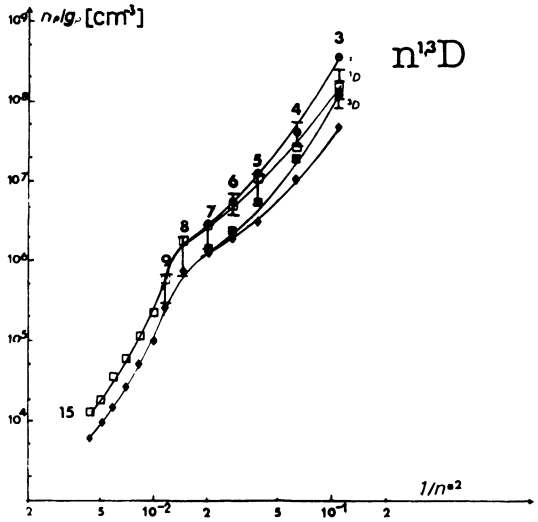

Fig. 4c. — Boltzmann diagrams for the levels $n\,^3$D and $n\,^1$D extended to $n = 20$. Comparison between the experimental densities (I) and the best fits computed with our C.R.M. at 50 mA and $P_{He} = 4.5$ torr. The lower curves (■, ◆) correspond to $T_e = 32\,000$ K, $n_e = 4 \times 10^{11}$ cm^{-3} and $N_1 = 1.27 \times 10^{17}$ cm^{-3} and the upper ones (●, □) to $T_e = 34\,000$ K, $n_e = 5 \times 10^{11}$ cm^{-3} and $N_1 = 1.41 \times 10^{17}$ cm^{-3}.

particules are taken into account by Allis. These processes increase when the gas pressure decreases. Consequently, the ionization rates must increase when the pressure decreases, thus counterbalancing the growth of the losses by diffusion of electrons or of metastables. Therefore, the electron temperature must be larger.

Moreover, Von Engel and Steenbeck [70] give some universal curves of electron temperature in terms of the product $c.p.R.$ where p is the gas pressure, $R = \phi/2$

the discharge radius and c a constant dependent on the nature of the gas. This theory gives 120 000 K at 1 torr and 48 000 K at 4.5 torr in disagreement with our extimates of 55 000 K and 33 000 K respectively. In this theory, the rate equation of electron density is

$$\frac{\partial n_e}{\partial t} = S n_e - n_e \frac{D_a}{\delta^2} \qquad (10)$$

where S is the electronic ionization frequency from the atomic ground state and D_a/δ^2 the ambipolar diffusion frequency, Volume recombination is neglected. In the stationary regime, $\partial n_e/\partial t = 0$ holds.

Because these authors neglect the ionization by inelastic collisions between metastable atoms, the associative ionization and step by step ionization by electronic collisions *via* excited states (so-called cascade ionization) their theory and our results disagree.

Taking into account these last processes, S is obtained from the population densities calculated by our C.R.M. for a given pressure, a given electron density and for various electron temperatures. On the other hand D_a/δ^2 is calculated as a function of T_e considering the decrease of the ambipolar diffusion coefficient with the electron energy according to Frost [71]. The intersection of the two curves ($S = f(T_e)$ and $D_a/\delta^2 = f(T_e)$) gives the electron temperature value for which (10) is checked. In this manner at 4.5 torr T_e is in good agreement with the values determined from the comparison between the calculated and measured population densities.

In the theory of Von Engel and Steenbeck [70], S is independent of n_e and $S = D_a/\delta^2$. Consequently, the electron temperature is not dependent on the electronic density. But when the other ionization processes are considered, T_e becomes a function of n_e. In particular, the frequency of stepwise ionization depends on the population densities of the excited states which are also functions of n_e.

Figure 5 shows an example of the variation of T_e with n_e from the solution of the (10) in the range $10^{10} \leqq n_e\ (\mathrm{cm}^{-3}) \leqq 10^{13}$ at $P_{He} = 4.5$ torr. In this figure, the electron temperature value estimated by comparison between measured and calculated population densities (first method) is also shown ($4 \times 10^{11} \leqq n_e\ (\mathrm{cm}^{-3}) \leqq 5 \times 10^{11}$).

The variation of the contributions of some ionization processes with n_e is shown in figure 6. In this figure Γ_1, Γ_2 and Γ_3 are the frequencies of respectively, ionization due to electronic collisions from the ground state, atomic collisions involving two metastable atoms, and associative ionization, where

$$\Gamma_1 = n(1\,^1\mathrm{S})\, S(1\,^1\mathrm{S})$$

$$\Gamma_2 = h[n(2\,^3\mathrm{S})\, n(2\,^3\mathrm{S}) + n(2\,^3\mathrm{S})\, n(2\,^1\mathrm{S}) + n(2\,^1\mathrm{S})\, n(2\,^1\mathrm{S})]/n_e$$

$$\Gamma_3 = \frac{1}{n_e}\left[\sum_p S^N(p)\, n(p)\, n(1\,^1\mathrm{S})\right].$$

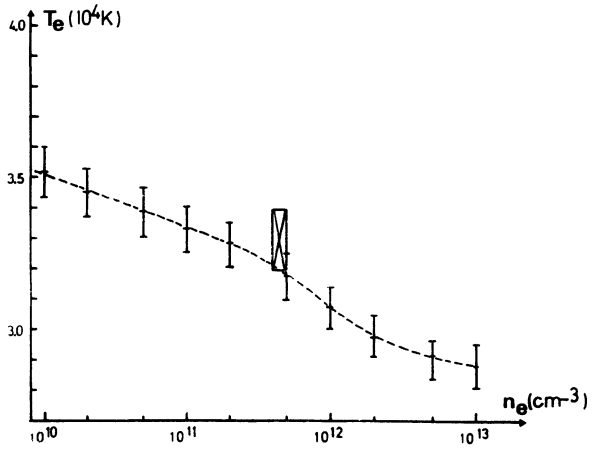

Fig. 5. — I The electron temperature T_e plotted as a function of n_e and determined from (10) for n_e in the range 10^{10} cm^{-3} to 10^{13} cm^{-3}. ⊠ Estimation of T_e by comparison between computed and experimental population densities at $P_{He} = 4.5$ torr and for $4 \times 10^{11} \leqq n_e(\mathrm{cm}^{-3}) \leqq 5 \times 10^{11}$.

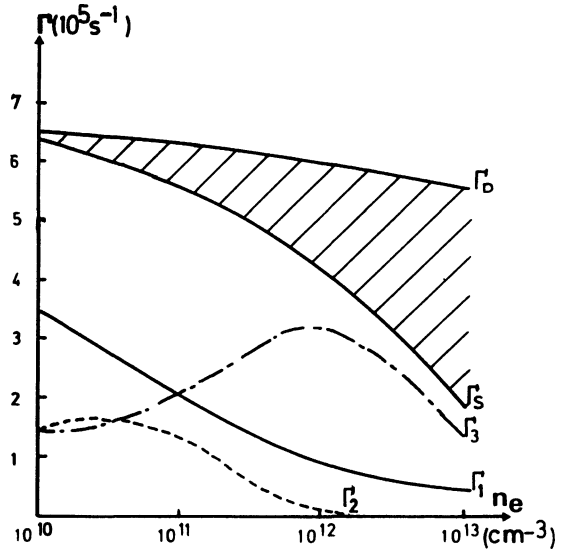

Fig. 6. — Ionization frequencies Γ_i of various ionization processes at $P_{He} = 4.5$ torr as a function of n_e. Γ_1 : electronic collisions with ground state atoms. Γ_2 : atomic collisions involving two metastable atoms. Γ_3 : associative ionization. Γ_S : $\Gamma_1 + \Gamma_2 + \Gamma_3$, $\Gamma_D = D/\Lambda^2$ ambipolar diffusion frequency.

In figure 6, the sum $\Gamma_S = \Gamma_1 + \Gamma_2 + \Gamma_3$ and the diffusion frequency $\Gamma_D = D_a/\delta^2$ are also plotted as functions of n_e. The difference between Γ_D and Γ_S illustrated by the dashed area, can be understood as the frequency of electronic stepwise ionization. The figure clearly shows that this ionization process increases with n_e. Then, at high electron densities, it can be expected that the ionization of helium atoms is mainly caused by electronic collisions in two or more steps.

Table II. — *Calculated population densities of* $n\,^3S$ *levels* (cm^{-3}) *at* T_e = 52 000 K, 54 000 K *and* 60 000 K *and corresponding experimental values* (Exp) (*Read* 6.3 11 = 6.3 × 10^{11}).

	52 000 K	54 000 K	60 000 K	Exp.
n(2 S)/g	6.3 11	7.33 11	9.9 11	6.3 ± 1.5 11
n(3 S)/g	7.08 8	8.42 8	1.25 9	6.4 ± 2.0 8
n(4 S)/g	8.34 7	1.00 8	1.56 8	7.9 ± 2.4 7
n(5 S)/g	1.41 7	1.71 8	2.79 7	1.9 ± 0.65 7
n(6 S)/g	6.12 6	7.42 6	1.29 7	5.9 ± 2.1 6

According to figure 5, T_e decreases when n_e increases. Hence, firstly, the averaged electron kinetic energy is too weak to induce ionization by electronic collisions either directly or in two steps *via* the metastable states ($n(2\,^3S).S(2\,^3S) = 10^4\ s^{-1}$ at $n_e = 10^{13}\ cm^{-3}$). Secondly, for $n_e \geqq 10^{12}\ cm^{-3}$, the excited states are mainly populated by electronic collisions from the ground state and by n-changing collisions (Fujimoto [7]). Consequently, electron collision ionization in several steps is probably the leading ionization process at high electron densities.

5.2 COMPARISON WITH EXPERIMENTAL RESULTS OF FUJIMOTO. — Hook's method was used by Fujimoto *et al.* [72] to measure the population densities of the $n = 2$ sublevels in a helium discharge 8 mm in radius and 0.4 torr in pressure. The electron temperature (57 000 K) and the electron density (6.3 × $10^{10}\ cm^{-3}$) were calculated with his model (Fujimoto [7]) for a discharge current of 100 mA.

His results and those obtained with our C.R.M. for the same conditions are plotted on figure 7. Good agreement is observed between the two sets of results. However the electron density and temperature values estimated by Fujimoto do not fit (10).

Beside, many pairs of $n_e - T_e$ values can be chosen that give the same $n = 2$ sublevel population densities. This is an illustration of the difficulty in determining the electron temperature by comparing too small a number of measured population densities with the calculated ones. This last remark can be applied to the method used by Brenning [73] in the determination of electron temperature from the comparison of the relative intensities of two lines. It must be noted that atom-atom collisions are not included in his model. For $P_{He} > 1$ torr, these processes modify the relative populations of the $n = 3$ sublevels and thus, the relative line intensities used to determine T_e.

5.3 OTHER RESULTS. — In a previous paper [30] the C.R.M. was used to study the excitation transfers induced by electronic collisions involving the helium atomic levels $5 \leqq n \leqq 8$. Experimentally, the levels $n \geqq 8$ were photoionized by CO_2 laser irradiation on the discharge 2.5 mm in diameter and 0.8 torr in helium pressure for n_e ranging from $10^{13}\ cm^{-3}$ to

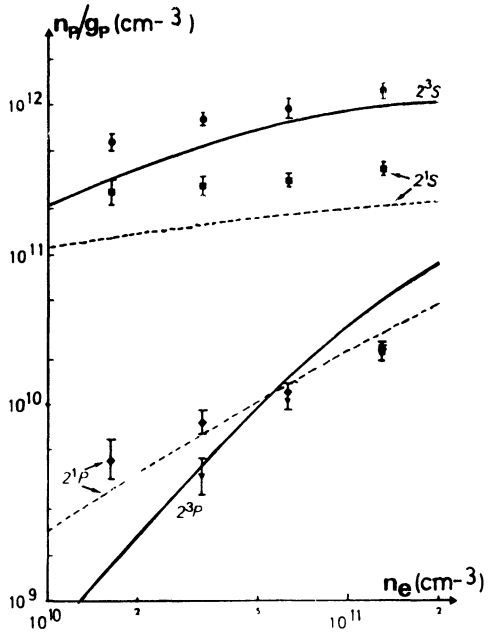

Fig. 7. — Comparison between the population densities of level $n = 2$ computed with our C.R.M. (continuous and dashed curves) and those measured by Fujimoto [72] ($\bar{\mathbf{1}}$ 2 ^{3}S, $\bar{\mathbf{1}}$ 2 ^{1}S, $\bar{\mathbf{1}}$ 2 ^{1}P, $\bar{\mathbf{1}}$ 2 ^{3}P) as a function of n_e at T_e = 57 000 K.

$5 \times 10^{13}\ cm^{-3}$. By comparing the absolute values of measured population densities of atomic excited states to the ones calculated with our C.R.M., an electron temperature (53 000 ± 2 000 K) and an electron density (1.5 ± 0.4 × $10^{13}\ cm^{-3}$) were determined. This electron density was confirmed by a measurement of the Stark broadening of the H_β line.

6. Conclusion.

A good quantitative knowledge of a large number of elementary processes in the helium atomic system at low pressure is necessary to build a collisional radiative model (C.R.M.). In addition to the conventional processes (radiative decay and electronic collisions) our C.R.M. takes in account the atomic collisions. The atomic collision cross-sections used are deduced from experimental data of B. Dubreuil and A. Catherinot [17-19], which is an original feature of our work. Moreover all the sublevels $|n, L, S\rangle$ for $1 \leqq n \leqq 7$ and all the levels $|n\rangle$ for $8 \leqq n \leqq 20$ are considered in the C.R.M. which as usual allows a more complete description of the physical behaviour.

Particularly, our C.R.M. yields the determination of the electron temperature T_e in capillary glow discharge plasma, where its measurement is practically impossible by other methods. The electron densities and temperatures obtained always verify the electron rate equation (Eq. (10)) that states that diffusion losses equal gains by volume ionization. A study of this balance equation shows that ionization by colli-

sions involving two metastable atoms and associative ionization from all other excited states cannot be neglected when the working pressure is larger than 2 torr.

Finally the determination of the electron density and electron temperature by comparing too small a number of measured excited state population densities with those calculated from our C.R.M. appears to us to be doubful.

Acknowledgments.

The authors are grateful to B. Dubreuil and A. Catherinot for interesting discussions and comments.

References

[1] Bates, D. R., Kingston, A. E., McWhirter, R. W. P., *Prov. R. Soc.* **267** 297 ; **270** (1962) 155.
[2] Bates, D. R., Kingston, A. E., *Planet Space Soc.* **11** (1963) 1.
[3] Drawin, H. W., Emard, F., *Physica C* **85** (1977) 333.
[4] Drawin, H. W., Emard, F., Tables of reduced population coefficients for the levels of atomic helium. Report EUR-CEA-FC-697 Association Euratom-CEA. Fontenay-aux-Roses (1973) (See also EUR-CEA-FC-534 (1970)).
[5] Deloche, R., Thèse d'Etat, Paris VI (1976).
[6] Hess, R., Burell, F., *J. Quant. Spectros. Radiat. Transfer* **21** (1979) 23.
[7] Fujimoto, T., Fukuda, K., *J. Phys. Soc. Japan* **50** (1981) 3476.
[8] Hedge, M. S., Ghosh, P. K., *Physica* **97C** (1979) 275.
[9] Strivastava, J. M. C., *J. Quant. Spectros. Radiat. Transfer* **25** (1981) 59.
[10] Catherinot, A., Thèse d'Etat, Orléans, France (1979).
[11] Catherinot, A., Sy, A., *Z. Naturforschung* **30a** (1975) 1143.
[12] Sayer, B., Jeannet, J. C., Berlande, J., *J. Physique* **33** (1972) 993.
[13] Drawin, H. W., Emard, F., Dubreuil, B., Chappelle, J., *Z. Plasmaphysik* **14** (1974) 103.
[14] Drawin, H. W., *Z. Naturforsch* **19a** (1964) 1451.
[15] Drawin, H. W., Klan, F., Ringler, H., *Z. Naturforschung Band* **26a** (1971) 2.
[16] Drawin, H. W., *Z. Physik* **211** (1968) 404.
[17] Dubreuil, B., Catherinot, A., *Phys. Rev. A* **21** (1980) 188.
[18] Catherinot, A., Dubreuil, B., *Phys. Rev. A* **23** (1981) 763.
[19] Catherinot, A., Dubreuil, B., Gousset, G., *Phys. Rev. A* **21** (1980) 618.
[20] Gauthier, J. C., Devos, F., Delpech, J. F., *Phys. Rev. A* **14** (1976) 2182.
[21] Devos, F., Boulmer, J., Delpech, J. F., *J. Physique* **40** (1979) 215.
[22] Biondi, M. A., *Phys. Rev.* **82** (1951) 453.
[23] Phelps, A. V., *Phys. Rev.* **99** (1955) 1307.
[24] Holstein, T., *Phys. Rev.* **72** (1947) 1212. *Phys. Rev.* **83** (1951) 1159.
[25] Irons, F. E., *J. Quant. Spectros. Radiat. Transfer* **22** (1979).
[26] Drawin, H. W., Emard, F., *Beitrague Plasmaphys.* **13** (1973) 143.
[27] Van den Eynde, P. K., Wiedes, G., Niemeyer, T., *Physica* **59** (1972) 401.
[28] Abrams, R. L., Volga, G. J., *Phys. Rev. Lett.* **19** (1967) 1411.
[29] Johnson, L. C., Hinnov, G., *Phys. Rev.* **187** (1969) 143.
[30] Gousset, G., Pignolet, P., Dubreuil, B., *Electronic excitation transfer cross section between helium atomic excited states n = 5, 6, 7 and 8.* 6 Abstracts of the ESCAMPIG 1982 (European Physical Society, 1982).
[31] Gingerich, O., Proc. 1st Harvard Smithsonian Conf. on Stellar Atmospheres, 17 Cambridge (Massachus.) (1964). Edited by Smithonian Institution, Astrophysical Observatory, Cambridge (Massachus.).
[32] Drawin, H. W., *Collision and Transport cross sections.* Report EUR-CEA-FC 383 (1966). Association Euratom CEA Fontenay-aux-Roses.
[33] Dubreuil, B., Chapelle, J., *Physica* **94C,** 233 (1978).
[34] Bates, D., Damgaard, A., *Philos. Trans. A* **242** (1949) 101.
[35] Burell, C. F., Kunze, H. J., *Phys. Rev. A* **18** (1978) 2081.
[36] St John, R. M., Miller, F. L., Lin, C. C., *Phys. Rev.* **134** (1964) 1888
[37] Jobe, J. D., St John, R. M., *Phys. Rev.* **164** (1967) 117.
[38] Moustafa Moussa, H. R., De Heer, F. J., Schutte, J., *Physica* **40** (1969) 517.
[39] Van Raan, A. F. J., Dejongh, J. P., Van Eck, J., Heidemann, H. G. M., *Physica* **53** (1971) 45.
[40] Hall, R. I., Joyez, G., Mazeau, J., Reinhardt, J., Schermann, C. S., *J. Physique* **34** (1973) 827.
[41] McCann, K. J., Flannery, M. R., *Phys. Rev. A* **10** (1974) 2264.
[42] Scott, T., McDowell, M. R. C., *J. Phys. B.* **9** (1976) 2235.
[43] Strivastava, R., Rai, D. K., *J. Phys. B.* **11** (1978) 309.
[44] Baluya, K. L., McDowell, M. R. C., *J. Phys. B.* **12** (1979) 835.
[45] Bhadra, K., Callaway, J., Henry, R. J. W., *Phys. Rev. A* **19** (1979) 1841.
[46] Wersterreld, W. B., Heidemann, H. G. M., Van Eck, J., *J. Phys. B.* **12** (1979) 115.
[47] Fon, W. C., Berrington, K. A., Kingston, A. E., *J. Phys. B.* **13** (1980) 2309.
[48] Vriens, L., Simpson, J. A., Mielczarek, S. R., *Phys. Rev.* **165** (1968) 7.
[49] Van Raan, A. F., Van Eck, J., *Phys. Rev. A* **13** (1976) 1276.
[50] Trajmar, S., *Phys. Rev. A* **8** (1973) 191.
[51] Ton That, D., Manson, S. J., Flannery, M. R., *J. Phys. B.* **10** (1977) 621.
[52] Roy, A. C., Sil, N. C., *J. Phys. B.* **12** (1979) 497.
[53] Fon, W. C., Berrington, K. A., Burke, P. G., Kingston, A. E., *J. Phys. B.* **14** (1981) 2921.

[54] FON, W. C., BERRINGTON, K. A., BURKE, P. G., KINGSTON, A. E., *J. Phys. B.* **12** (1979) 1861.
[55] FLANNERY, M. R., MCCANN, K. J., *Phys. Rev. A* **12** (1975) 846.
[56] OCHKUR, V. I., BRATSEV, V. F., *Sov. Astronomy AJ* **9** (1966) 797.
[57] KHAYRALLAH, G. A., CHEN, S. T., RUMBLE, J. R., *Phys. Rev. A* **17** (1978) 513.
[58] MARIOTT, R., *Proc. Phys. Soc.* **87** (1966) 407.
[59] JOHNSON, L. C., *Astrophys. J.* **174** (1972) 227.
[60] VRIENS, L., SMEETS, A. H. M., *Phys. Rev. A* **22** (1980) 940.
[61] BOULMER-LEBORGNE, C., GOUSSET, G., IXth Colloque sur la Physique des Collisions Atomiques et Electroniques, Nice (France) (1982). (See also C. BOULMER-LEBORGNE, Thèse de spécialité, Orléans (France) 1982.) (Edited by C.E.A. Saclay.)
[62] ALLIS, W. P., *Les fonctions de distribution*, Rapport Interne, Laboratoire de Physique des Gaz et des Plasmas, Orsay, France (1972).
[63] DUBREUIL, B., CATHERINOT, A., *Ann. Phys.* **7** (1982) 359.
[64] PENNEL, A., 9e Colloque sur la Physique des Collisions Atomiques et Electroniques, Nice (France) (1982). (Edited by C.E.A. Saclay.)
[65] JOHNSON, A. W., GERARDO, J. B., *Phys. Rev. A* **7** (1973) 925.
[66] MORGAN, J. E., SCHIFF, H. I., *Can. J. Chem.* **2042** (1964) 1300.
[67] MARTINS, W. C., *J. Research N.B.S.* **64** (1960) 1.
[68] RALSTON, A., WILE, H. S., *Math. Methods for digital computers.* (John Wiley and sons, Inc., New York.) 1960.
[69] MITCHELL, A. G. G., ZEMANSKY, M. W., *Resonant Radiation and excited atoms.* (Camber Un. Press., N.Y.) 1961.
[70] VON ENGEL, A., STEENBECK, M., *Elektrische Gasentladungen VII. J.* (Springer, Berlin) 1932.
[71] FROST, L. S., *Phys. Rev.* **105** (1957) 354.
[72] FUJIMOTO, T., MIYAZAKI, K., FUGUDA, K., *J. Quant. Spectros. Radiat. Transfer* **14** (1974) 377.
[73] BRENNING, N., *J. Phys. D* **13** (1980) 1459.
[74] DELOCHE, R., MONCHICOURT, P., CHERET, M., LAMBERT, F., *Phys. Rev. A* **13** 3 (1976) 1140.